Article:
Shirazi, H.A., Lee, S. orcid.org/0000-0002-0797-1446, Ullah, S. et al. (1 more author) (2024) Structural and tribological studies on the interaction of porcine gastric mucin with non- and cationic-modified β-lactoglobulins. Colloids and Surfaces B: Biointerfaces, 238. 113924. ISSN 0927-7765

https://doi.org/10.1016/j.colsurfb.2024.113924

Structural and tribological studies on the interaction of porcine gastric mucin with non- and cationic-modified β-lactoglobulins

Hadi Asgharzadeh Shirazi[1], Seunghwan Lee[1,2*], Saif Ullah[3], Kristoffer Almdal[3]

[1]Department of Mechanical Engineering, Technical University of Denmark, DK-2800, Kgs. Lyngby, Denmark

[2]Institute of Functional Surfaces, School of Mechanical Engineering, University of Leeds, LS2 JT9, The United Kingdom

[3]Department of Chemistry, Technical University of Denmark, DTU Chemistry, DK-2800 Kgs. Lyngby, Denmark

*Corresponding author: email) S.Lee4@leeds.ac.uk

Abstract

β-lactoglobulin (BLG) is the major whey protein with negative charges at neutral pH in aqueous media. Thus, the interaction with mucins, the major polyanionic component of mucus, is very weak due to the electrostatic repulsion between them. The present study postulates that cationization of BLG molecules may reverse the interaction characteristics between BLG and mucin from repulsive to associative. To this end, cationic-modified BLGs were prepared by grafting positively charged ethylenediamine (EDA) moieties into the negatively charged carboxyl groups on the aspartic and glutamic acid residues and compared with non-modified BLG upon mixing with porcine gastric mucin (PGM). To characterize the structural and conformational features of PGM, non/cationized BLGs, and their mixtures, various spectroscopic approaches, including zeta potential, dynamic light scattering (DLS), and circular dichroism (CD) spectroscopy were employed. Importantly, we have taken surface adsorption with optical waveguide lightmode spectroscopy (OWLS), and tribological properties with pin-on-disk tribometry at the sliding interface as the key approaches to determine the interaction nature between them as mixing PGM with polycations can lead to synergistic lubrication at the nonpolar substrate in neutral aqueous media as a result of an electrostatic association. All the spectroscopic studies and a substantial improvement in lubricity collectively supported a tenacious and associative interaction between PGM and cationized BLGs, but not between PGM and non-modified BLG. This study

demonstrates a unique and successful approach to intensify the interaction between BLG and mucins, which is meaningful for a broad range of disciplines, including food science, macromolecular interactions, and biolubrication etc.

Keywords: Mucin; β-lactoglobulin; Cationization; Biotribology; Biolubrication.

1. Introduction

A mucosa or mucus membrane is the soft tissue that lines the organs interfacing external world such as the buccal cavity [1-3], ocular [4], respiratory [5], reproductive [6], and gastrointestinal [7] tracts to protect and lubricate the underlying epithelial cells. The protective functions of mucus membranes are achieved by secreting biological lubricants like tear film, saliva, and phlegm, which can be classified as mucus. The major non-water macromolecular component of mucus is mucin which consists of a heavily glycosylated central region and unglycosylated N-/C-terminus by way of a linear protein backbone chain [8] and are negatively charged at neutral pH. Inherent lubricity of mucus has made it so noteworthy that many investigations have been devoted to the biotribological characteristics of mucus lubrication [9-11]. Accordingly, many investigations have focused on the lubricating properties of its major component i.e., mucin as well [12-19]. Since the low elastic modulus of polydimethylsiloxane (PDMS) (1-4 MPa) allows for a soft contact analogous to living systems [12-19], a self-mated PDMS interface was employed in the above-mentioned studies to assess the lubricating capabilities in aqueous solution. Lee et al. [15] revealed porcine gastric mucin (PGM) could be an effective aqueous lubricant additive under specific conditions of acidic pH and low ionic strength. Nevertheless, PGM is generally known to be a poor lubricant additive in dilute concentration (≤ 1 mg/mL) at neutral pH [17-19]. Interestingly, mixing of PGM with some polycations such as polyallylamine hydrochloride (PAH) [9], poly-l-lysine (PLL) [9], polyethylenimine (PEI) [9] (both linear and branched) [9,10] and chitosan [11] have been reported to display considerable synergistic lubricating effect [9-11]; the coefficient of friction (μ) of either PGM or polycation alone was reduced by two orders of magnitude in low-speed regime (e.g., at 0.25 mm/s) upon mixing them. A strong electrostatic attraction between negatively charged PGM and positively charged polycations was an important key factor in improving the slippery characteristics [9-11].

Although these studies provide an excellent demonstration of polymeric mucoadhesive interaction to display synergistic lubrication, few studies are available for interactions between mucins and proteins in the same context [16]. Interactions of mucins and proteins are abundant in nature such as in human and animal saliva and tears, chicken eggs, and dairy products. Thus, a better understanding of mucin and protein complexation on the molecular level is of great importance to divulge valuable information on the critical parameters affecting the natural interaction between them [20,21]. In this study, we intend to investigate whether a similar synergistic lubricating effect from PGM/polycations is to be identified from the interaction between PGM and proteins.

β-lactoglobulin (BLG) is one of the most important proteins of dairy food systems that has received considerable interest in the areas of food oral processing and digestion, particularly in association with saliva [2,3]. BLG is a 162-residue globular protein with a molecular weight of 18.3 kDa, representing approximately 60% of bovine whey protein. Previous studies have shown incorporating BLG solution into whole saliva [22] or bovine submaxillary mucin [3, 23] exhibited no apparent synergistic lubricating effect, even at different pH values of ~3, ~5, and ~7. This finding suggests that the native BLG is unable to establish a strong aggregate with mucin, especially under cyclic tribostresses. A lack of an electrostatic attraction between negatively charged BLG and mucin molecules can be assumed to be the primary reason for the weak interaction between BLG and mucin. A native BLG molecule possesses 16 lysine, 3 arginine, 10 aspartic acid, and 16 glutamic acid residues [24]. These anionic amino acid residues result in an overall negatively charged BLG, and thus PGM and BLG may rather repel each other from an electrostatic interaction perspective. Here we note that substituting cationic moieties (e.g., ethylenediamine (EDA)) for such anionic amino acid residues of BLG can be associated with a highly positive surface charge [25,26]. This can play a substantial role in the complexation between BLG and mucin or mucus via electrostatic attraction. In the present study, we propose that in addition to the characterization of structural and conformational changes, the characterization of tribological properties can provide an important insight into the potential complexation between PGM and non-/cationic-modified BLG solutions (at pH~7.0). To assess the tribological properties, a pin-on-disc tribometry was employed at a hydrophobic self-mated PDMS tribopair. An array of structural and conformational measurements including dynamic light scattering (DLS), and zeta (ζ) potential, circular dichroism (CD) spectroscopy, and optical

waveguide light mode spectroscopy (OWLS) were also performed on the solution samples. This study discloses that the cationization of BLG has a paramount effect on the mucoadhesive properties of BLG and the slippery nature of mucins.

2. Materials and methods

2.1. Mucin

PGM (Type III, bound sialic acid 0.5-1.5%, partially purified powder) was purchased from Sigma-Aldrich (Denmark, Brøndby) and used as received. To prepare the PGM stock solution, PGM was dispersed in an aqueous buffer solution (PBS) at 1 mg/mL concentration. After centrifuging at 6,000 rpm for 15 min., the precipitated parts were discarded, and only dissolved parts were used for further experiments.

2.2 β-lactoglobulin (BLG) and cationization of BLG

BLG variant A was purified from cow's milk as described previously [27]. The purity of the sample was verified by analytical ultracentrifugation. The anionic carboxylic groups on the aspartic and glutamic acid residues of native BLG were treated with EDA in the presence of N-(3-dimethylaminopropyl)-N-ethylcarbodiimide (EDC), as described earlier [25]. The process of cationization was achieved via a previously reported carbodiimide-catalyzed reaction mechanism [28]. For this purpose, 400 mg of BLG was dissolved in 5 mL Milli-Q water at mild stirring speed. To the dissolved BLG solution, 50 mL of EDA solution at three different concentrations (0.5, 1.0 and 1.5 mol/L) was added and the final solution was kept stirring. The pH of the BLG-EDA solution was adjusted to 4.75 with 1 M HCl and equilibrated for half an hour. The process of cationization was initiated by adding 150 mg of EDC and kept at slow stirring for 2 hours. Then, the reaction was terminated by adding 540 µL of 4 M sodium acetate buffer and at a pH of 4.75. The cationized BLG, along with some unreacted particles, was dialyzed against Milli-Q water at 4 °C for 48 hours and further freeze-dried.

The molecular weights (M_Ws) of BLG and cationized BLG were determined by matrix-assisted laser desorption/ionization time-of-flight (MALDI-TOF) mass spectrometry (Bruker Daltonics) in the linear mode. Sample solutions were 1mg/mL of each protein in H_2O and matrix solution was sinapic acid (10 mg/mL) in acetonitrile with 0.05% trifluoroacetic acid. 0.5 µL matrix

solution was placed on the sample holder and dried, followed by addition of 0.5 μL of sample solution and dried. Finally, another 0.5 μL matrix solution was placed and dried. Please note that the unmodified BLG gives rise to a sharp peak in the MS-spectrum whereas the modified samples M1BLG, M2BLG, and M3BLG show a molecular weight distribution, and thus the specified number of modified units represents the mean number of modified units. A summary is provided in Table 1 below, although further details will be published somewhere else. The chemicals used in the cationization of BLG were purchased from Sigma-Aldrich (Europe) including EDA dihydrochloride (98% purity) and EDC (97% purity).

2.3. Zeta potential and dynamic light scattering (DLS) measurements

Zeta (ζ) potential and dynamic light scattering experiments were conducted on PGM, non-/cationic-modified BLG, and their mixture solutions with a ZETASIZER NANO instrument (Model ZEN5600, Malvern Instruments Ltd., UK). Disposable folded capillary cells (Model DTS1070, Malvern Instruments Ltd., UK) and Dip Cell Kit (Model ZEN1002, Malvern Instruments Ltd., UK) were utilized for DLS and zeta (ζ) potential experiments, respectively. Before both DLS experiments, cuvettes, and the electrode were cleaned with Hellmanex® III, Millipore water, and ethanol and then blown-dried with nitrogen. The DLS instrument analyzed each solution for at least five runs and each run averaged ten measurements. The results of both ζ potentials and hydrodynamic sizes are presented with the statistical information below (average and error bars). But, for hydrodynamic size distribution, the averaged plots over multiple measurements will be presented. ζ potential and size distribution of solutions were determined, respectively, based on electrophoretic mobility and phase analysis light scattering using DLS analyzer software (i.e., Zetasizer 7.11).

2.4. Circular dichroism (CD) spectroscopy

CD spectra were monitored with a Chirascan spectrophotometer (Applied Photophysics Ltd, Surrey, UK) at room temperature. Far-UV and near-UV CD spectra were recorded in the wavelength ranges of 280-190 nm and 400-200 nm, respectively. For both far-/near-UV CD, a step size of 1 nm and a bandwidth of 1 nm were pre-set. All solutions, with constant concentration i.e., 1 mg/mL, were scanned three times and the average of scans is presented.

2.5. Pin-on-disk tribometry and tribopair

μ vs. speed plots were acquired for all solutions with a pin-on-disk tribometer (CSM, Peseux, Switzerland) using a PDMS-PDMS tribopair. To perform a pin-on-disk experiment, an array of pre-sets including load (F_N = 1 N), fixed disk track (R = 4 mm), and temperature (T = 25°C) was defined. A loaded PDMS pin was slid over a fixed track of the PDMS disk, which was placed in a cell containing the specific amount (2 mL) of the solutions. The sliding friction force (F_F) between the pin and the disk was measured using a strain gauge. The mean and standard deviation (SD) values of μ, as defined as F_F/F_N (F_N = normal force), were calculated by the tribometer software (Tribometer module/Version 4.4.M, InstrumX) in response to varying sliding speed in the range of 0.25 to 100 mm/s.

In the present pin-on-disk tribometry configuration, PDMS pins and disks were prepared by mixing the base fluid and crosslinker of Sylgard 184 elastomer kit (Dow Corning, Midland, MI) at a ratio of 10:1 under a gentle vacuum. The resultant mixture was then poured into the pin-/disk-shape molds and allowed to cure at 70°C overnight. The entire pin-on-disk tribometry experiments were measured three times, and the average values with error bars are presented.

2.6. Optical waveguide lightmode spectroscopy (OWLS)

An OWLS 210 Label-free Biosensor system (Microvacuum Ltd, Budapest, Hungary) was employed to measure the adsorbed mass of the solutions onto PDMS surface during specific time. To this end, waveguides (200-nm thick $Si_{0.25}Ti_{0.75}O_2$ waveguiding layer on 1 mm thick AF 45 glass, Microvacuum Ltd, Budapest, Hungary) were spin-coated with a preliminary ultrathin layer (about 30 nm [13]) of polystyrene (at 2500 rpm for 15 s). Afterwards, a subsequent ultrathin layer of PDMS was spin-coated at 2000 rpm for 25 s. Polystyrene was prepared at 6 mg/mL in toluene and PDMS was prepared by dissolving PDMS mixtures, including base fluid and crosslinker, in hexane at a ratio of 10:3 (final concentration of 0.5% w/w). Spin-coated waveguides were placed into an oven at 70°C overnight.

During OWLS experiment, a programmable syringe pump (Model 1000-NE, New Era Pump Systems, Inc., NY) was linked to the device to move buffer solutions through the flow cell containing the OWLS waveguide surface. In the first step, it allowed the buffer solution to pass through the waveguide surface until a stable baseline reached. Next, 100 µL of the solution sample

was fed into the flow cell utilizing a loading loop. Upon observing an increase in the adsorbed mass graph, the pump was paused for 15 min to accomplish adsorption process in a static situation. Finally, the pump was re-started to rinse the flow cell with buffer and then the adsorbed mass was calculated according to Feijter's equation. Beforehand, the refractive index increment (dn/dc) values for the solution samples were experimentally determined using an automatic refractometer (Rudolph, J157) and input into the analyzer. The (dn/dc) values of PGM, M0BLG, PGM/M0BLG, M3BLG and PGM/M3BLG solutions were equal to 0.13, 0.22, 0.18, 0.15 and 0.14 cm^3/g respectively. For each sample, the measurements were performed three times, and the average values and error bars of adsorbed masses are presented.

3. Results and discussion

3.1 Characterization of cationized BLGs

Cationization of BLG was carried out by varying the amount of reacting EDA, yielding BLGs with three different levels of cationic residues. The M_Ws of the cationized BLGs and the number of cationic residues in the modified BLG as characterized by MALDI-TOF mass spectroscopy are shown in Table 1.

Table 1. The M_Ws of the cationized BLGs and the number of cationic residues in the modified BLG as characterized by MALDI-TOF mass spectroscopy.

	M_W (Da)	Difference	Number of modified residues
M0BLG	18360.9	-	
M1BLG	18771.1	410.2	9.3
M2BLG	18822.4	461.5	10.5
M3BLG	19052.3	691.4	15.7

The cationized BLG samples are denoted as M1BLG, M2BLG, and M3BLG according to the extent of cationization and the number of cationic residues. It should be noted that the numbers 1, 2, 3 in the notations M(i)BLG (i = 1, 2, 3) were chosen according to the ranking of cationization,

but they do not scale with the exact extent of cationization. As a reference, non-modified BLG is denoted as M0BLG. It should be noted that the estimated number of positive residues is notably higher for M3BLG compared to M1BLG and M2BLG.

3.2. Zeta (ζ) potential of the solutions

As the surface characteristics of PGM and BLG aggregates can be exposed to change upon mixing, ζ potential measurement is one of the best ways to acquire useful information on the molecular-level interaction. In this regard, ζ potential values of PGM, non-/cationic-modified BLG, and their mixture are listed in Table 2. Both PGM and M0BLG exhibited strong negative surface charges, i.e., -22.00 ± 1.28 and -24.06 ± 0.64 mV, respectively. These values were consistent with previous investigations for PGM [12,15] and BLG [3,23,25,26,29]. The isoelectric point of BLG is known to be pH~5 [29,30]. Therefore, it is reasonable to expect the strong negative value of ζ potential for BLG at pH~7. For the PGM/M0BLG mixture (ratio 1/1 (w/w)), a strong negative value of ζ potential (-22.72 ± 0.93 mV) was obtained, close to those of the individual components. On the other hand, all cationic-modified BLG showed positive ζ potentials. As the degree of cationization increased, the ζ potential shifted toward a more positive value. The more positively charged EDA moieties were grafted into the negative carboxyl groups, the higher the value of ζ potential attained. Regarding this upward trend of ζ potential, M3BLG indicated the highest value of ζ potential (26.37 ± 3.64 mV) compared to the other modified BLGs. It is noted though that the relationship between the number of EDA units added to BLG and ζ potential is not linear; the difference in the number of EDA units on M1BLG and M2BLG is small (9.3 and 10.5, respectively), but the difference in ζ potential between them (3.78 mV on average) is rather comparable to that between M2BLG and M3BLG (3.89 mV on average), although M3BLG has a much higher number of EDA units (15.7). Given that there are a total of 26 carboxylic acids (from 10 aspartic acid and 16 glutamic acid residues) to react with EDA units [24], the exact sources of carboxylic acids, and their locations on BLG, could be different, which can lead to a noticeable difference in zeta potential despite similar number of EDA units as in M1BLG and M2BLG. A clarification on the relation between the number of EDA unis and zeta potentials is left to future studies involving multiple batches of cationized BLGs and characterizations. With mixing PGM to the modified BLG (ratio 1/1 (w/w)), the absolute values of ζ potential significantly decreased by rising the degree of cationization, insofar as both PGM/M2BLG (-3.96 ± 0.30 mV) and

PGM/M3BLG (1.65 ± 1.18 mV) had near-zero net charge. In fact, strong positive charges of M2-/3-BLGs could almost completely cancel out the negative charge of PGM and it may indicate the activation of electrostatic attraction between them. Nevertheless, it should be cautioned that ζ potential measurements do not provide a stand-alone conclusion about the interaction nature between PGM and BLGs, because in principle, a simple mixture between them without any associative interaction may lead to a similar result. The nature of interaction between PGM and BLG was further investigated by probing the changes in hydrodynamic size distribution of the sample solutions, which will be discussed in the following section.

Table 2. Mean and SD values of ζ for all solutions.

Solution	**ζ potential (mV)**
PGM	-22.00 ± 1.25
M0BLG	-24.06 ± 0.64
PGM/M0BLG	-22.72 ± 0.93
M1BLG	18.70 ± 1.34
PGM/M1BLG	-9.78 ± 0.53
M2BLG	22.48 ± 1.38
PGM/M2BLG	-3.96 ± 0.30
M3BLG	26.37 ± 3.64
PGM/M3BLG	1.65 ± 1.18

3.3. Hydrodynamic size distribution

Figure 1 indicates the volume-weighted distribution of the hydrodynamic diameter (D_H) for PGM, non-/cationic-modified BLGs, and their blend. PGM was characterized by a bimodal size distribution with two local maxima at around 351 ± 35 nm and 2.4 ± 0.5 μm. PGM inherently tends to form a self-aggregation in an aqueous medium and, as a result, shows a high polydispersity in size distribution [12-15]. Moreover, non-mucin biomolecules in commercially available PGM may

be responsible for multiple peaks over the wide range of D_H values either as free impurity fragments or as linkers between PGM molecules. On the other hand, all BLG solutions exhibited a tiny size (below 6 nm in D_H), considerably less than PGM. M0BLG (unmodified BLG), with an average hydrodynamic diameter of 5.6 ± 0.2 nm, had a good agreement with those reported previously [25,29-31].

Upon mixing PGM and M0BLG (ratio 1/1 (w/w)), a new peak that is very close to PGM in size population appeared (Figure 1(a)), suggesting that the size distribution of PGM was not significantly affected as a result of mixing with M0BLG. This behavior was expected due to the lack of electrostatic attraction between negatively charged PGM and M0BLG molecules. However, it is also observed that the M0BLG peak (ca. 5.6 nm) completely disappeared in the mixture solution and the major PGM peak slightly shifted toward a smaller size. One possibility of a small shrinkage of PGM molecules is that PGM and M0BLG could establish other weaker interactions than electrostatic attraction such as hydrogen bonding [2,3]. One can also argue that the changes in mixed solution are mostly indebted from the dominance of larger particles in the multi-disperse mixture, i.e., a sort of technical artifact. This can certainly be a cause for the disappearance of the BLG peak, but not the slight shrinking of the PGM peak at the same time. Thus, even though some small BLG molecules may remain free without being detected by DLS analysis, PGM and BLG appear to interact with each other, leading to shrinkage of PGM. Analogous to M0BLG, cationic BLGs also showed molecular sizes of less than 6 nm in diameter (Figure 1(b) – (d)). After mixing PGM and cationic BLG solutions (ratio 1/1 (w/w)), the peaks of cationic BLGs also disappeared and the major peak of PGM tended downward to lower D_H values. But the magnitude of peak shift is much more significant for PGM-cationic BLGs (Figure 1(b) – (d)) than PGM-M0BLG (Figure 1(a)), which suggests that the interaction mechanism for this pair is possibly different and stronger. Furthermore, the magnitude of contraction of PGM after interaction with cationic BLG is roughly proportional to the degree of cationization of BLG. Based on the distinct opposite surface charges of PGM and cationic BLGs (Table 2), it is reasonable to propose that electrostatic attraction plays a dominating role in the interaction between PGM and cationic BLG molecules. This tenacious electrostatic interaction caused a substantial shrinkage in D_H of PGM [12-14] so that M3BLG could dramatically drop PGM size from 2.4 ± 0.5 μm (before complexation) to 704 ± 23 nm (after complexation).

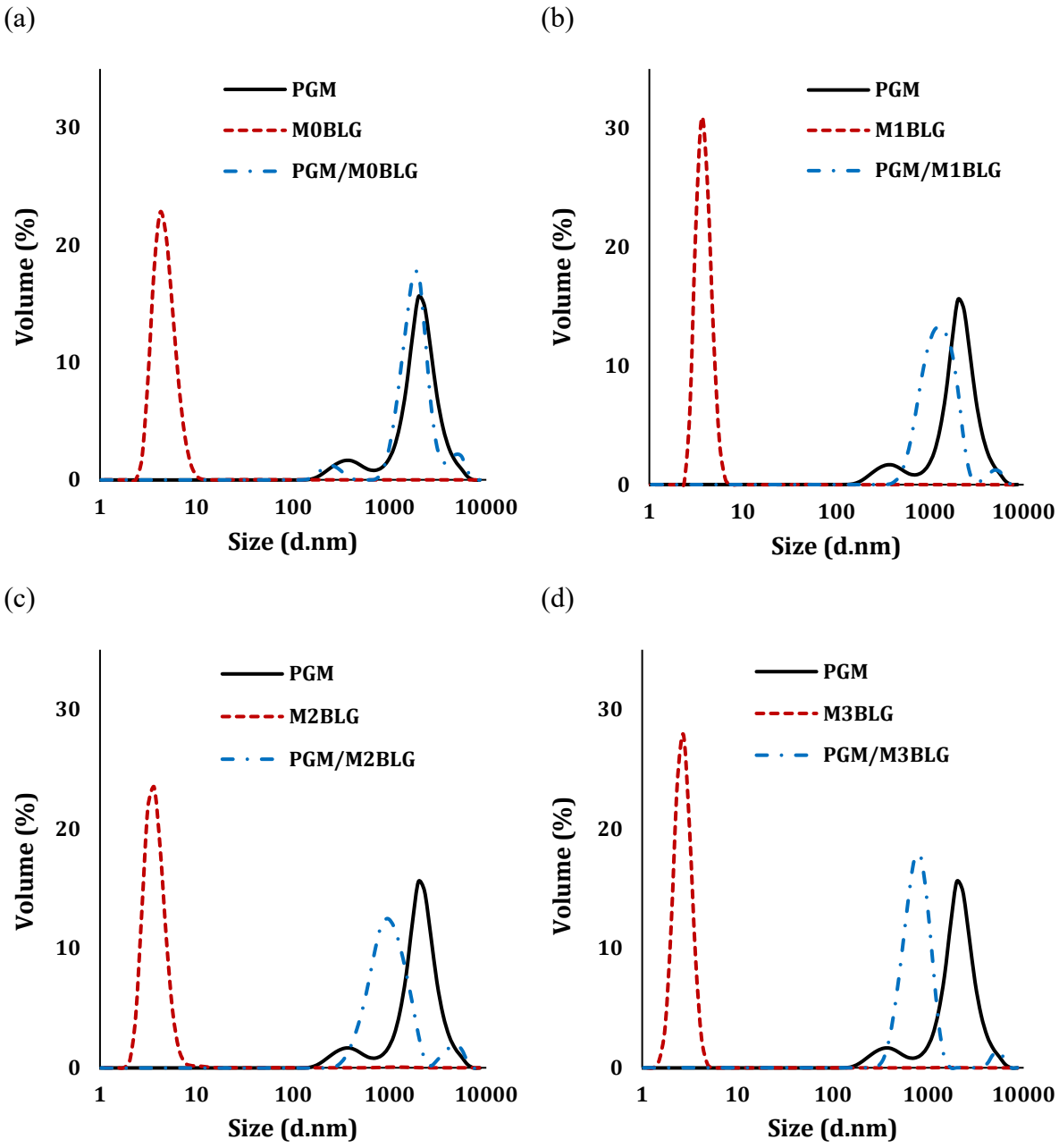

Figure 1. Volume-weighted distribution of the hydrodynamic diameter DH for either individual or mixed components of (a) PGM:M0BLG, (b) PGM:M1BLG, (c) PGM:M2BLG and (d) PGM:M3BLG solutions.

3.4. Changes of secondary and tertiary structures: conformational study

The far-UV CD spectra of all solutions including non-/cationic-modified BLG (Figure 2(a)), PGM (Figure 2(b)), and their mixtures (Figure 2(b), ratio 1/1 (w/w)) at pH~7 were plotted in Figure 2. The far-UV spectrum of the PGM solution illustrated a broad negative peak with a minimum at around 207 nm, reflecting a broadly defined random coil structure [32]. The far-UV spectrum of M0BLG revealed a negative peak around 215 nm, indicating the dominance of a well-defined antiparallel β-sheet structure [33]. In addition, the intensity of the negative peak of M0BLG is larger than that of PGM roughly by three times, which is probably due to the higher molar concentration of M0BLG compared to PGM under the same concentration of 0.5 mg/mL. It is interesting to note that the far-UV CD spectrum of BLG is slightly, yet clearly altered upon cationization; the intensity of the negative peak (near 215 nm) in far-UV CD spectra is somewhat reduced for M1BLG and M2BLG, although the location of negative peak did not change noticeably. This slight weakening of β-sheet structure may be closely associated with the consumption of glutamic and aspartic acids, existing mainly in β-sheet parts of M0BLG, during the cationization process [25]. In contrast, M3BLG showed a slight shift to a lower wavelength (~209 nm) in the location of the negative peak without a noticeable reduction in intensity. This change may occur from the weakened β-sheet structure after a high degree of conjugation of EDA moieties into amino acid backbone [34] and the formation of relatively more flexible structures e.g., helices, turns, and coils, than β-sheets [25]. Such flexibility of M3BLG could be a favorable addition to electrostatic attraction to facilitate its interaction with PGM molecules or PDMS substrate. Lastly, the difference between the far UV CD spectra of M3BLG compared to M1BLG/M2BLG further supports that the structural features of M3BLG are qualitatively different from those of M1BLG/M2BLG due to the distinctively higher extent of cationization (Table 1).

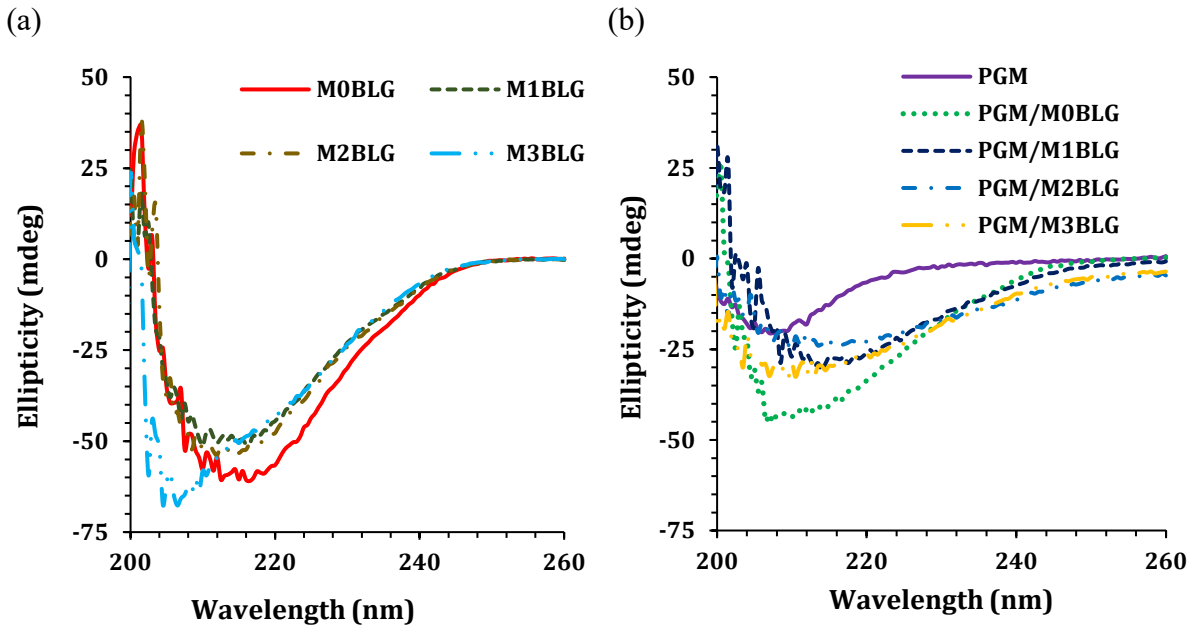

Figure 2. Secondary structure measurement: far-UV spectra of (a) M(*i*)BLG, (b) PGM and its mixture with M(*i*)BLG (*i* = 0, 1, 2, and 3). The horizontal axes of far-UV CD graphs started at 200 nm due to very high noise in the spectra at lower wavelengths.

The near-UV CD spectra of PGM and BLGs are presented in Figure 3. The most distinctive feature was a single positive peak observed from PGM with a maximum of around 270 nm. This peak (between 250 nm to 280 nm) may be closely associated with the tertiary structure surrounding aromatic side chains of PGM, located exclusively at the C- and N-terminals [35]. In contrast to far-UV CD spectra, all BLG molecules (Figure 3(a)) showed much weaker intensities than PGM (Figure 3(b)) in their near-UV CD spectra. M0BLG near-UV spectrum showed three sharp peaks at ~274, ~283 and ~293 nm. These distinct troughs may also be associated with the chirality involving the aromatic amino acids side chain related to the tryptophan, tyrosine, phenylalanine, and disulfide bonds existence in M0BLG [36-38]. A band observed at ~274 nm was possibly owing to phenylalanyl residues, and both occupied at ~283 nm and ~293 nm reflected tryptophanyl residues of M0BLG [36,39]. After modification of BLG with EDA, a decline in the intensity of three deep peaks in near-UV spectra was observed. While the primary effect of the cationization of BLG with EDA is to impart positive charges, it also increases the surface hydrophobicity due to the addition of $–CH_2CH_2-$ units to the BLG surface. The tertiary structure of peptides or proteins

is typically distinct when hydrophobic patches are well preserved but is weakened when they are exposed to the surface. These reductions probably came from the changes in the environment of tryptophan [40]. Nevertheless, it should be stressed again that despite some features observed from the near-UV CD spectra of non/cationic-modified BLGs (Figure 3(a)) as addressed above, their intensities are clearly weaker than those of PGM (Figure 3(b)).

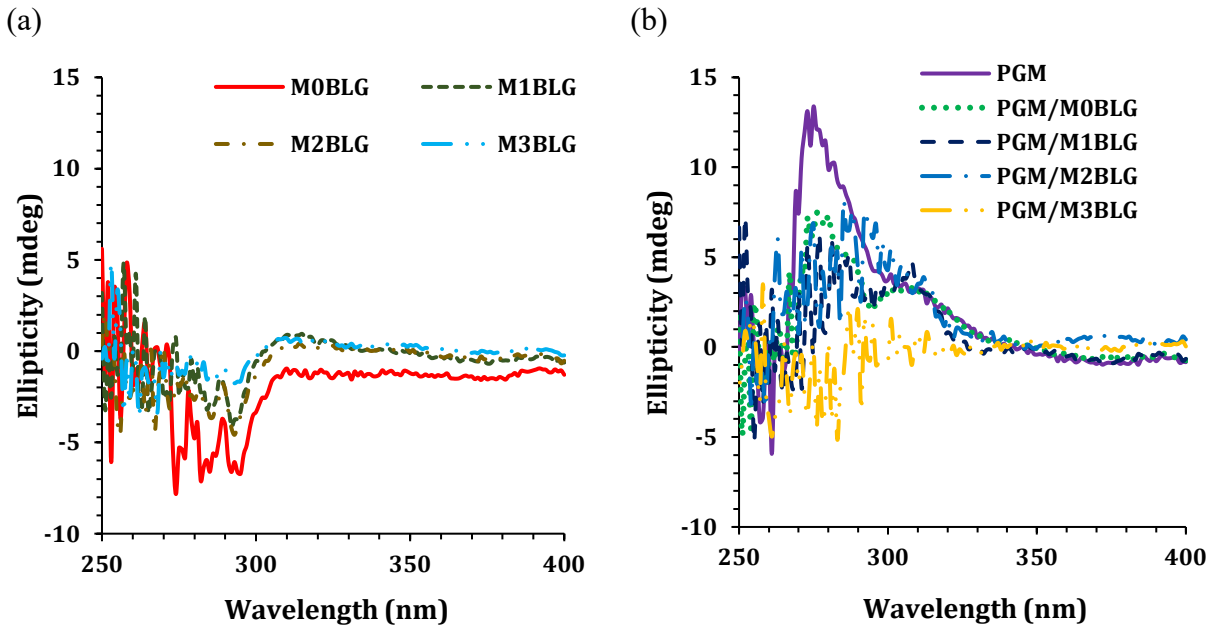

Figure 3. Near-UV spectra of (a) M(*i*)BLG, (b) PGM and its mixture with M(*i*)BLG (*i* = 0, 1, 2, and 3).

For both far-UV (Figure 2) and near-UV (Figure 3) CD spectra, all the solutions of PGM and non/cationic-modified BLG mixtures revealed qualitatively intermediate features between those of PGM alone and respective BLG. But it is also notable from Figure 2(b) that the far-UV CD spectrum for PGM/BLG (M0BLG) mixture is most distinctively different from those of PGM/cationic-modified BLG mixtures, further suggesting that the changes in the secondary structures as a result of the interaction between PGM and non-modified BLG are clearly different from that between PGM and cationic-modified BLGs. On the other hand, the extent of changes in near-UV CD spectra after mixing PGM and BLGs, i.e., the changes in tertiary structures as a result of the interaction between PGM and BLGs were most pronounced for the PGM/M3BLG pair.

Meanwhile, all the other pairs were some intermediates between respective spectra of PGM and each BLG solution and were virtually indistinguishable from each other (Figure 3(b)).

In previous studies where PGM and polycations were mixed to drive a synergistic lubricity [12-14], CD spectroscopy was employed as a technical means to visualize the associative interaction between them. If the two types of macromolecules were simply co-present in the mixture solution without associative interaction, the CD spectrum of a mixture of PGM-polycation should match with that of a calculated average of each solution, i.e. $S_{Mix} = S_{AVG}$, where S_{Mix} is the CD spectrum of the mixed solution of PGM and polycations and $S_{AVG} = ½\cdot(S_{PGM} + S_{POL})$, where, in turn, S_{PGM} is the CD spectrum of PGM solution and S_{POL} is the CD spectrum of polycation prior to mixing. Meanwhile, a strong discrepancy between S_{Mix} and S_{AVG} suggests a strong association between PGM and polycations as mixing them leads to an aggregate between them. This approach was fairly straightforward in those studies because polycations were featureless in both far-UV and near-UV CD spectra. In the present case though (the resultant spectra are provided in Figure S1 (far-UV) and Figure S2 (near-UV) in the Supplementary Material), both PGM and BLG have strong secondary and tertiary structures as reflected in the far-UV and near-UV CD spectra as shown in Figures 2 and 3. Thus, the interpretation of the same comparison is not straightforward as both proteins affect each other in a complicated manner. Nevertheless, it can be at least deduced that as the experimental far-UV (Figure 4) and near-UV (Figure 5) CD spectra of PGM/M(i)BLG mixture and the calculated average of individual spectra were clearly different, the two proteins interact and distort the original conformation of each.

3.5. Adsorption of PGM-M(0-/3-)BLG exemplars onto PDMS surface

In the OWLS approach, it was attempted to emulate the surface adsorption conditions of the macromolecules under tribostress by setting a limited exposure time (ca. 15 min) even though this is typically not sufficient to reach a surface adsorption equilibrium. During pin-on-disk tribometry, adsorption/removal/(re)adsorption of the specimen molecules and aggregates onto PDMS is repeatedly established due to the cyclic tribostress. Surface adsorption properties of PGM, cationized BLG, and their mixtures onto PDMS surface may provide further information on the interaction between PGM and cationized BLG. In this study, M3BLG was exploited as a representative cationized BLG to form a mixture solution with PGM. M0BLG was also employed

as a control. Figure 4 presents the adsorbed masses per unit area for PGM, M0BLG, M3BLG, PGM/M0BLG (ratio 1/1 (w/w)), and PGM/M3BLG (ratio 1/1 (w/w)) solutions onto PDMS surface spin-coated on OWLS waveguides (see section 2.6.). As can be observed from this figure, PGM showed a highly adsorbed mass value which was in line with those reported in Refs. [12,13]. Meanwhile, M0BLG displayed poor adsorption behavior onto the PDMS surface. This difference can be firstly ascribed to the much larger M_W of PGM than BLG but is also affected by the presence of distinct nonpolar patches for PGM, which act as anchoring units to nonpolar PDMS surfaces [15,41-43]. The adsorbed areal mass of the PGM-M0BLG mixture was also much lower than PGM but was higher than that of M0BLG by a narrow margin. These features of M0BLG and PGM-M0BLG solutions (pH~7) were consistent with a previous surface adsorption study investigated with another technique [23]. This behavior of the PGM/M0BLG mixture was attributed to two features. Firstly, M0BLG molecules were smaller and lighter than PGMs. Therefore, M0BLG could migrate onto the PDMS surface in an aqueous medium more quickly than PGM, especially on the short adsorption time scale in this study (i.e., 15 min, namely "Vroman effect" [44]). Secondly, by considering the equilibrium between PGM and M0BLG from the standpoint of weight/volume concentration in the mixture solution (0.5 mg/mL for each), M0BLG molecules outnumbered PGMs and contributed to the dominant adsorption of M0BLG over PGM. Most importantly, the low adsorbed areal mass of PGM-M0BLG in the mixture supports that PGM and M0BLG molecules do not have a strong interaction to formulate aggregates.

On the other hand, M3BLG solution exhibited higher adsorbed mass than M0BLG (Figure 4). As Teng et al. demonstrated in the previous study, cationic modification of BLG by incorporating EDA leads to an increase not only in the positive surface charges but also in the surface hydrophobicity mainly due to the presence of $–CH_2CH_2-$ units in EDA [25]. Thus, an increment in the adsorbed mass of M3BLG can be attributed to its increased surface hydrophobicity compared to M0BLG and more facile interaction with hydrophobic PDMS surface in aqueous environment [45]. Moreover, in contrast to the PGM-M0BLG mixture, the PGM-M3BLG mixture displayed a substantially higher areal mass, even slightly higher than that of PGM. As with other cases in the adsorption of PGM/polycation mixtures onto PDMS surface in previous studies [12-14], neutralization in surface charge of PGM/M3BLG upon formation of tenacious aggregates appears to be mainly responsible for the facilitated adsorption onto nonpolar

PDMS surface, although hydrophobic interaction between PGM and M3BLG might have augmented their interactions to a certain extent.

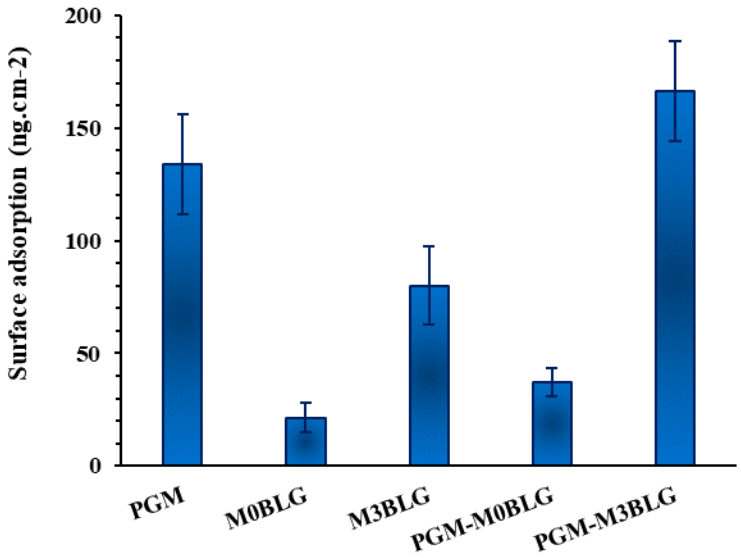

Figure 4. Adsorbed mass values of PGM, M0-/3-BLG and their mixture solutions onto PDMS-coated waveguides. The adsorption time was 15 min.

3.5. Lubricating properties: pin-on-disk tribometry

In order to test the hypothesis that cationized BLG molecules may behave like other polycations and synergistically enhance the lubricity of PGM [12-14], M3BLG, the most positively charged BLG, was firstly employed to formulate mixed solutions with PGM at varying weight ratios. Figure 5 displays μ vs. speed plots of PGM:M3BLG as a function of the weight fraction of M3BLG solution with respect to the total weight of PGM-M3BLG mixture solution as well as some control solutions.

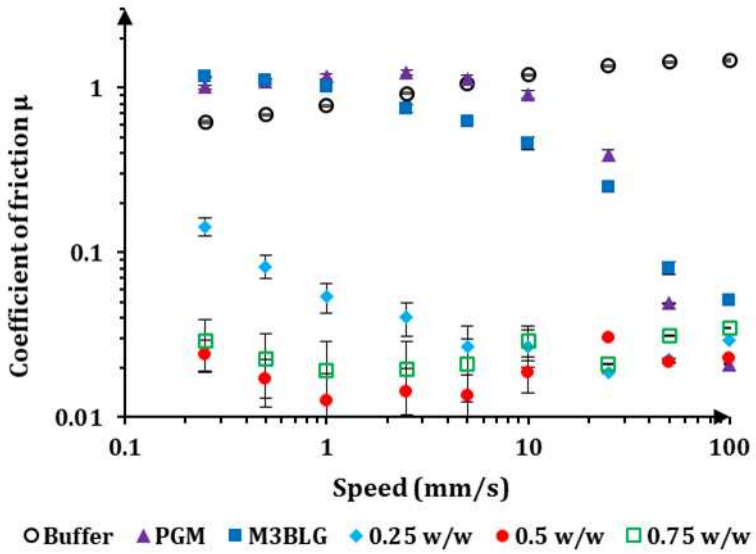

Figure 5. Changes in μ of PGM:M3BLG, solutions with varying weight fraction of M3BLG (w/w) over the sliding speed range of 0.25-100 mm/s using pin-on-disk tribometry at the PDMS-PDMS surfaces.

Both PGM and M3BLG solutions exhibited very poor lubricating capabilities in that the μ values were close to those of the sliding contacts of PDMS-PDMS in the HEPES buffer, except for in the high-speed regime (speed ≥ 50 mm/s). Thus, both PGM and M3BLG commonly displayed high amounts of surface adsorption (Figure 4), yet poor lubricity (Figure 5) at the PDMS surface in a neutral aqueous solution. Upon mixing PGM with M3BLG, μ significantly decreased in the whole speed range compared to those of their individual components i.e., PGM and M3BLG, even from when the weight ratio for M3BLG is only 0.25. Moreover, an enhanced reduction in μ values was observed from the mixture of 0.5 w/w M3BLG, especially in the low-speed regime (< ca. 10 mm/s). However, a further decreasing trend in μ with an increasing ratio of M3BLG is saturated at 0.5 and a further increase of M3BLG such as 0.75 w/w did not further improve the lubricity. Based on the observations from the PGM-M3BLG mixture solution (Figure 5), the μ vs speed plots of all the mixture solutions, i.e., PGM:M(i)BLG (i = 0, 1, 2, and 3) were compared at the weight ratio of 0.5 w/w as shown in Figure 6.

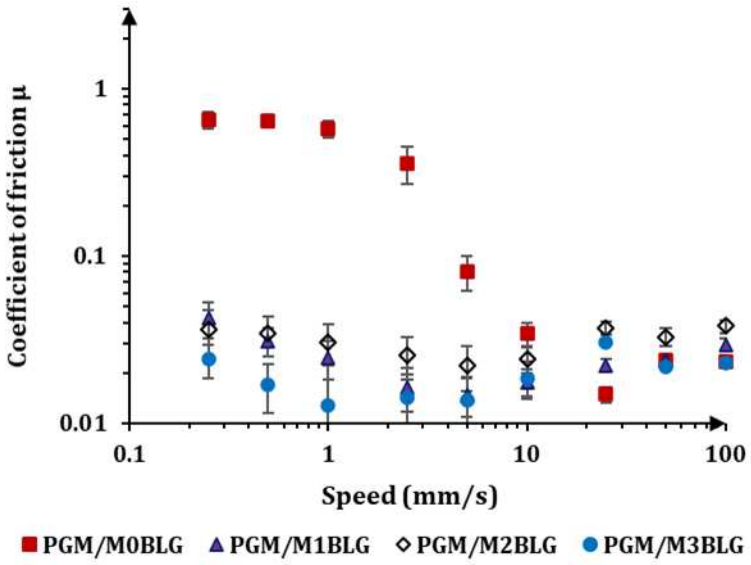

Figure 6. Changes in μ of the mixture solutions (w/w = 0.5) of PGM and M(i)BLG (i = 0, 1, 2 and 3) in response to the sliding speed range of 0.25-100 mm/s using pin-on-disk tribometry on the PDMS-PDMS surfaces.

Friction-lowering effect for PGM/M0BLG compared to its constituent proteins, namely PGM or M0BLG alone, was negligible. In contrast, all PGM-cationized BLG mixtures showed lower μ values than those of PGM/M0BLG by more than an order of magnitude in low-speed regime (≤ 2 mm/s), indicating the improvement in boundary lubrication properties upon mixing PGM with cationized BLG. This observation supports that mixing of PGM and cationized BLG leads to a strong associative interaction between them, as opposed to a simple mixing solution. It is interesting to note that the overall behavior of cationized BLG is somewhat different from another cationic protein that was recently studied in the context of synergistic lubrication with PGM, namely lysozyme [16]; in the case of lysozyme, associative interaction between PGM and lysozyme, and eventually an effective synergistic lubrication, was not observed until lysozyme was heated at 90 °C for a moderate and optimum duration of time (e.g., 1 hour). Lysozyme that was either intact or heated for too long a duration of time (e.g., 6 hours) did not provide an optimal structural/conformational condition of the protein to interact with PGM because of, for instance, a strong self-assembly between lysozymes (intact) or excessive conformational changes after mixing with PGM (heating at 90 °C for 6 hours) [16]. In contrast, cationized BLGs remain predominantly as uimers (Figure 1) with the positive charges (Figure 2) and readily interact with PGM without

any pretreatments. Thus, it is reasonable to conclude that cationized BLG molecules behave very similarly with the polycations in previous studies, namely PEI [12,13] and chitosan [14], in that mixing with PGM leads to a significantly enhanced lubricity at a neutral and compliance tribological interface, such as PDMS-PDMS tribopair, without any pre-treatments.

4. Conclusion

In this study, the effects of the molecular-level interaction between PGM and non-/cationic-modified BLG on the surface charge, conformation, adsorption, and lubricating efficiency of the individual components and the mixture of PGM:BLGs were explored. A hydrophobic PDMS was employed to assess both adsorption and lubricating properties of the PGM, BLG proteins, and their mixtures. Both PGM and BLG evinced nearly negligible lubricating efficacy individually. In the mixture cases, apart from a poor lubricity of PGM/M0BLG, all PGM/cationic-modified BLG revealed an effective lubricating synergy, especially in the boundary lubrication regime. PGM:M(i)BLG (i = 1, 2, 3) exhibited a remarkable decrease of μ from ~1 for both PGM and M3BLG single components by nearly two orders of magnitude at the lowest sliding speed i.e. 0.25 mm/s. A distinctively lower friction forces observed from PGM:M(i)BLG (i = 1, 2, 3) compared to PGM:M0BLG is likely to have originated primarily from the presence of a strong electrostatic interaction for PGM:M(i)BLG (i = 1, 2, 3), but not for PGM:M0BLG. Additionally, increasing structural flexibility of BLG with increasing conjugation of EDA moieties into amino acid backbone from a "hard" protein structure of native BLG (e.g., M0BLG) could have contributed to facilitating its interaction with PGM molecules too. Based on the present and a recent study on the interaction of PGM and lysozyme [16], it can be deduced that the presence of distinct positive charges on proteins is definitely required to drive a strong association with PGM and synergistic lubrication, but it may be not sufficient depending on the systems. Further conditions appear to include flexibility in conformation and absence of self-aggregation as with some polycations [12]. Overall, this study has demonstrated that cationization of BLG can substantially improve the associative interaction with PGM and it can be exploited in a broad range of disciplines where the aggregation between mucins and BLG is favorable, such as food science, macromolecular interaction, and biolubrication etc.

Acknowledgements

The authors are grateful for the Danish Council for Strategic Research ("StrucSat", Grant no. 1308-00011B) for their financial support.

References

[1] Zheng Y, Bashandeh K, Shakil A, Jha S, Polycarpou AA, Review of dental tribology: Current status and challenges, Tribology International 2022, 166, 107354.

[2] Yılmaz H, Lee S, Chronakis IS, Interactions of β-lactoglobulin with bovine submaxillary mucin vs. porcine gastric mucin: The role of hydrophobic and hydrophilic residues as studied by fluorescence spectroscopy, Molecules 2021, 26(22), 6799.

[3] Çelebioğlu HY, Lee S, Chronakis IS, Interactions of salivary mucins and saliva with food proteins: A review, Critical Reviews in Food Science and Nutrition 2020, 60(1), 64-83.

[4] Mirea DA, Trunfio-Sfarghiu AM, Matei CI, Munteanu B, Piednoir A, Rieu JP, Blanchin MG, Berthier Y. Role of the biomolecular interactions in the structure and tribological properties of synovial fluid, Tribology International 2013, 59, 302-311.

[5] Linden SK, Sutton P, Karlsson NG, Korolik V, McGuckin, MA, Mucins in the mucosal barrier to infection, Mucosal Immunology 2008, 1(3), 183-197.

[6] Lagow E, DeSouza MM, Carson DD, Mammalian reproductive tract mucins, Human Reproduction Update 1999, 5(4), 280-292.

[7] Qu D, Wang G, Yu L, Tian F, Chen W, Zhai Q, The effects of diet and gut microbiota on the regulation of intestinal mucin glycosylation, Carbohydrate Polymers 2021, 258, 117651.

[8] Bansil R, Turner BS, Mucin structure, aggregation, physiological functions and biomedical applications, Current opinion in colloid & interface science 2006, 11(2-3), 164-170.

[9] Zhou Y, Huitink D, Liang H, Lubrication behavior of slug mucus, Materials Performance and Characterization 2012, 1, 1–8.

[10] Røn, T., Patil NJ, Ajalloueian F, Rishikesan S, Zappone B, Chronakis IS, Lee S, Gastric mucus and mucus-like hydrogels: Thin film lubricating properties at soft interfaces, Biointerphases 2017, 12, 051001.

[11] Wang X, Du M, Han H, Song Y, Zheng Q, Boundary lubrication by associative mucin, Langmuir 2015, 31, 4733–4740.

[12] Nikogeorgos N, Patil NJ, Zappone B, Lee S, Interaction of porcine gastric mucin with various polycations and its influence on the boundary lubrication properties, Polymer 2016, 100, 58-168.

[13] Patil, NJ, Rishikesan S, Nikogeorgos N, Guzzi R, Lee S, Zappone B, Complexation and synergistic boundary lubrication of porcine gastric mucin and branched poly (ethyleneimine) in neutral aqueous solution, Soft matter 2017, 13(3), 590-599.

[14] Nikogeorgos N, Efler P, Kayitmazer AB, Lee S, "Bio-glues" to enhance slipperiness of mucins: improved lubricity and wear resistance of porcine gastric mucin (PGM) layers assisted by mucoadhesion with chitosan, Soft Matter 2015, 11(3), 489-498.

[15] Lee S, Müller M, Rezwan K, Spencer ND, Porcine gastric mucin (PGM) at the water/poly (dimethylsiloxane) (PDMS) interface: influence of pH and ionic strength on its conformation, adsorption, and aqueous lubrication properties, Langmuir 2005, 21(18), 8344-8353.

[16] Shirazi HA, Lee S, Complexation between porcine gastric mucin (PGM) and lysozyme: Influence of heat treatment of lysozyme on the tribological properties, International Journal of Biological Macromolecules 2022, 203, 212-221.

[17] Cassin G, Heinrich E, Spikes HA, The influence of surface roughness on the lubrication properties of adsorbing and non-adsorbing biopolymers, Tribology Letters 2001, 11, 95–102.

[18] Nikogeorgos N, Madsen JB, Lee S, Influence of impurities and contact scale on the lubricating properties of bovine submaxillary mucin (BSM) films on a hydrophobic surface, Colloids and Surfaces B: Biointerfaces 2014, 122, 760-766.

[19] Schomig VJ, Kasdorf BT, Scholz C, Bidmon K, Lieleg O, Berensmeier S, An optimized purification process for porcine gastric mucin with preservation of its native functional properties, RSC Advances 2016, 6, 44932-44943.

[20] Hsein H, Garrait G, Beyssac E, Hoffart V, Whey protein mucoadhesive properties for oral drug delivery: mucin–whey protein interaction and mucoadhesive bond strength. Colloids and Surfaces B: Biointerfaces 2015, 136, 799-808.

[21] Dėdinaitė A, Claesson PM, Synergies in lubrication, Physical Chemistry Chemical Physics 2017, 19(35), 23677-23689.

[22] Vardhanabhuti B, Cox PW, Norton IT, Foegeding EA, Lubricating properties of human whole saliva as affected by β-lactoglobulin, Food Hydrocolloids 2011, 25(6), 1499-1506.

[23] Çelebioğlu HY, Gudjónsdóttir M, Chronakis IS, Lee S, Investigation of the interaction between mucins and β-lactoglobulin under tribological stress, Food Hydrocolloids 2016, 54, 57-65.

[24] Stein WH, Moore S, Amino acid composition of β-lactoglobulin and bovine serum albumin. Journal of Biological Chemistry 1949, 178, 79-91.

[25] Teng Z, Li Y, Luo Y, Zhang B, Wang Q, Cationic β-lactoglobulin nanoparticles as a bioavailability enhancer: protein characterization and particle formation, Biomacromolecules 2013, 14(8), 2848-2856.

[26] Teng Z, Li Y, Niu Y, Xu Y, Yu L, Wang Q, Cationic β-lactoglobulin nanoparticles as a bioavailability enhancer: Comparison between ethylenediamine and polyethyleneimine as cationizers, Food chemistry 2014, 159, 333-342.

[27] Kristiansen, KR, Otte J, Ipsen R, Qvist KB, Large-scale preparation of β-lactoglobulin A and B by ultrafiltration and ion-exchange chromatography. International Dairy Journal, 1998, 8(2), 113−118.

[28] Lu W, Zhang Y, Tan YZ, Hu KL, Jiang XG, Fu SK, Cationic albumin-conjugated pegylated nanoparticles as novel drug carrier for brain delivery, Journal of Controlled Release 2005, 107(3), 428–448.

[29] Çelebioğlu HY, Gudjónsdóttir M, Meier S, Duus JØ, Lee S, Chronakis IS, Spectroscopic studies of the interactions between β-lactoglobulin and bovine submaxillary mucin, Food Hydrocolloids 2015, 50, 203-210.

[30] Engelhardt K, Lexis M, Gochev G, Konnerth C, Miller R, Willenbacher N, Peukert W, Braunschweig B, pH effects on the molecular structure of β-lactoglobulin modified air–water interfaces and its impact on foam rheology, Langmuir 2013, 29(37), 11646-11655.

[31] Teng Z, Luo Y, Li Y, Wang Q, Cationic beta-lactoglobulin nanoparticles as a bioavailability enhancer: effect of surface properties and size on the transport and delivery in vitro, Food chemistry 2016, 204, 391-399.

[32] Kelly SM, Jess TJ, Price NC, How to study proteins by circular dichroism, Biochimica et Biophysica Acta-Proteins and Proteomics 2005, 1751(2), 119-139.

[33] Greenfield NJ, Using circular dichroism spectra to estimate protein secondary structure, Nature protocols 2006, 1(6), 2876-2890.

[34] De la Hoz L, Netto FM, Structural modifications of β-lactoglobulin subjected to gamma radiation, International Dairy Journal 2008, 18(12), 1126-1132.

[35] Kelly SM, Price NC, The use of circular dichroism in the investigation of protein structure and function, Current Protein and Peptide Science 2000, 1(4), 349-384.

[36] Kahn PC, The interpretation of near-ultraviolet circular dichroism. In Methods in enzymology 1979, 61, 339-378, Academic Press.

[37] Creamer LK, Effect of sodium dodecyl sulfate and palmitic acid on the equilibrium unfolding of bovine beta-lactoglobulin, Biochemistry 1995, 34(21), 7170-7176.

[38] Chevalier F, Chobert JM, Dalgalarrondo M, Choiset Y, Haertle T, Maillard glycation of β-lactoglobulin induces conformation changes, Food/Nahrung 2002, 46(2), 58-63.

[39] Strickland EH, Beychok S, Aromatic contributions to circular dichroism spectra of protein, CRC Critical Reviews in Biochemistry 1974, 2(1), 113-175.

[40] Reddy IM, Kella NK, Kinsella JE, Structural and conformational basis of the resistance of beta-lactoglobulin to peptic and chymotryptic digestion, Journal of Agricultural and Food Chemistry 1988, 36(4), 737-741.

[41] Bansil R, Stanley E, LaMont JT, Mucin biophysics, Annual Review of Physiology 1995, 57(1), 635-657.

[42] Shi L, Caldwell KD, Mucin adsorption to hydrophobic surfaces, Journal of Colloid and Interface Science 2000, 224(2), 372-381.

[43] Lindh L, Glantz PO, Carlstedt I, Wickström C, Arnebrant T, Adsorption of MUC5B and the role of mucins in early salivary film formation. Colloids and Surfaces B: Biointerfaces 2002, 25(2), 139-146.

[44] Vroman L, Adams AL, Findings with the recording ellipsometer suggesting rapid exchange of specific plasma proteins at liquid/solid interfaces, Surface Science 1969, 16, 438-446.

[45] Clark SL, Hammond PT, The role of secondary interactions in selective electrostatic multilayer deposition, Langmuir 2000, 16(26), 10206-10214.

[46] Rabe M, Verdes D, Seeger S, Understanding protein adsorption phenomena at solid surfaces, Advances in Colloid and Interface Science 2011, 162(1-2), 87-106.

SUPPLEMENTARY MATERIAL

Structural and tribological studies on the interaction of porcine gastric mucin (PGM) with non-/cationic-modified β-lactoglobulins

Hadi Asgharzadeh Shirazi[1], Seunghwan Lee[1,2], Saif Ullah[3], Kristoffer Almdal[3]

[1]Department of Mechanical Engineering, Technical University of Denmark, DK-2800, Kgs. Lyngby, Denmark

[2]Institute of Functional Surfaces, School of Mechanical Engineering, University of Leeds, LS2 JT9, The United Kingdom

[3]Department of Chemistry, Technical University of Denmark, DTU Chemistry, DK-2800 Kgs. Lyngby, Denmark

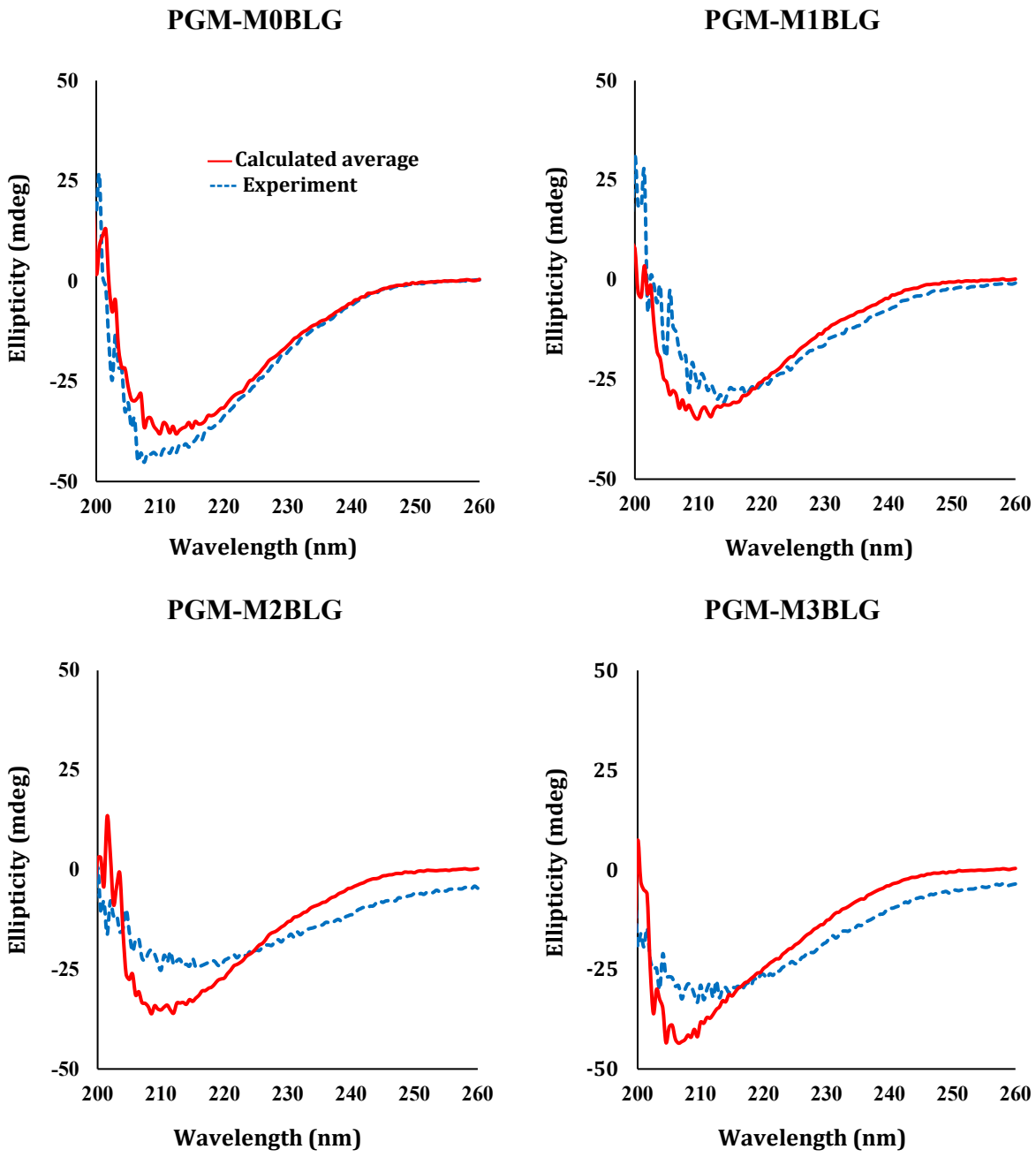

Figure S1. Far-UV spectra of numerical average vs. experimental data of PGM/M(*i*)BLG mixtures (*i* = 0, 1, 2, and 3). The horizontal axes of far-UV CD graphs started at 200 nm due to very high noise in the spectra at lower wavelengths.

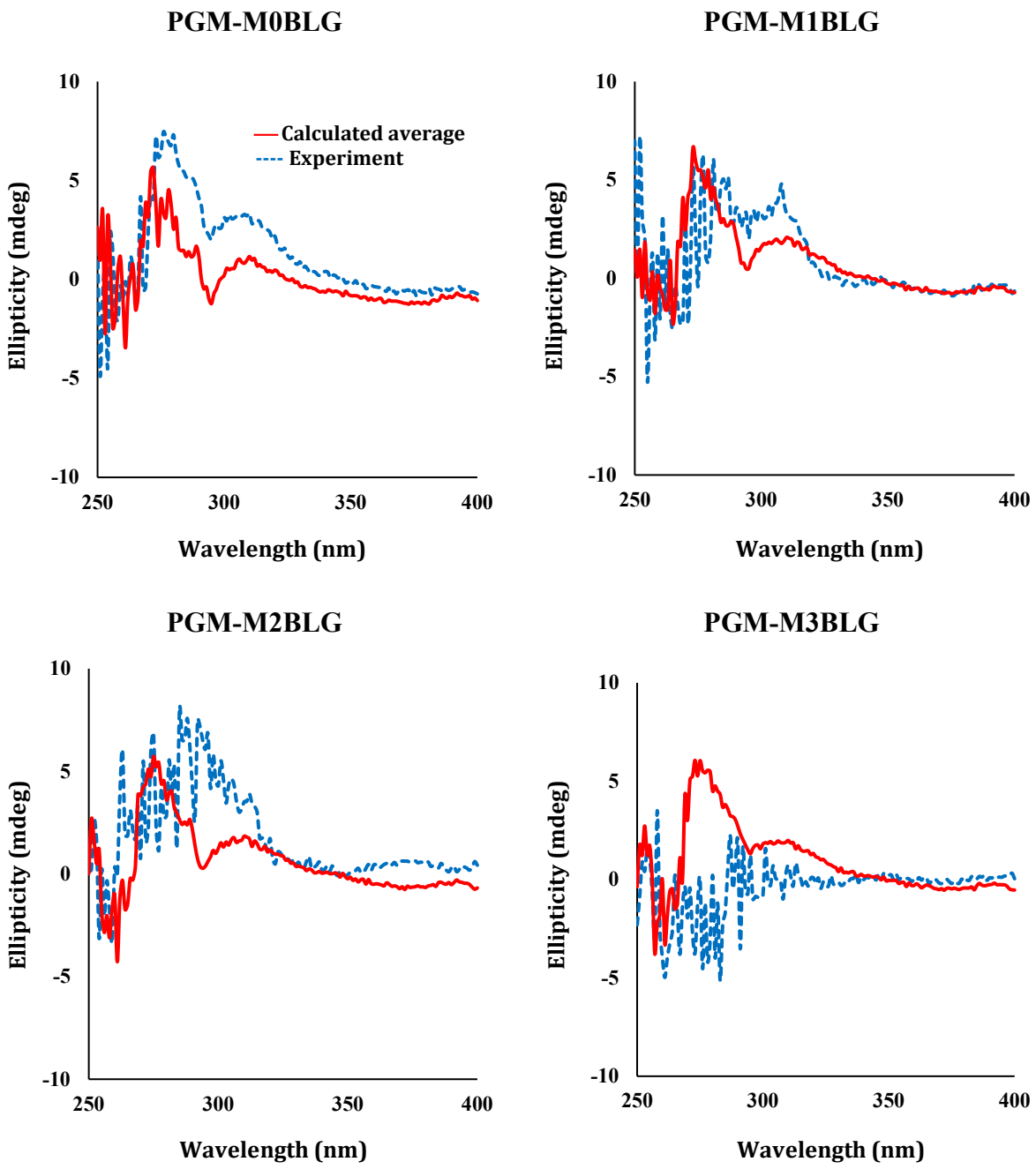

Figure S2. Near-UV spectra of numerical average vs. experimental data of PGM/M(*i*)BLG mixtures (*i* = 0, 1, 2, and 3).